

ARTICLE

OPEN



A take-home message from COVID-19 on urban air pollution reduction through mobility limitations and teleworking

Alba Badia¹, Johannes Langemeyer^{1,2,3}, Xavier Codina⁴, Joan Gilabert^{1,5,6}, Nacho Guilera⁴, Veronica Vidal^{1,7}, Ricard Segura¹, Mar Vives⁴ and Gara Villalba^{1,8}

The rigorous traffic limitations during COVID-19 have forced many people to work from home, reaching an outstanding degree of teleworking and reduction in air pollution. This exceptional situation can be examined as a large-scale pilot test to determine the potential of improving urban air quality through teleworking. Based on observed traffic reductions during the COVID-19 lockdown in Barcelona, we formulate socio-occupational scenarios, with various configurations of teleworking, and simulate them using the chemistry transport model WRF-Chem with multi-layer urban scheme. By intensifying teleworking to 2, 3, and 4 days a week, averaged NO_2 concentrations are reduced by 4% ($-1.5 \mu\text{g m}^{-3}$), 8% ($-3 \mu\text{g m}^{-3}$), and 10% ($-6 \mu\text{g m}^{-3}$), respectively, while O_3 increases moderately (up to $3 \mu\text{g m}^{-3}$). We propose that teleworking be prioritized and promoted as an effective contribution towards reduction of long-term urban air pollution and short-term pollution peaks.

npj Urban Sustainability (2021)1:35 ; <https://doi.org/10.1038/s42949-021-00037-7>

INTRODUCTION

The ongoing pandemic of coronavirus disease 2019 (COVID-19) has hit humanity hard and by surprise¹. To slow down the spread of the virus, radical measures have been implemented, among them an extraordinary limitation of people's movement—never seen to this extent at global scale². Under an imminent threat to human lives, scientific evidence, media warnings, bottom-up campaigns, and decisive political action have led to drastic measures to radically limit mobility as a way to mitigate the expansion of COVID-19. Now—as calls to return to 'normality' are becoming louder around the globe—we should raise some critical thought on which kind of normality we want to return to. Here we want to reflect upon lessons learned from the COVID-19 mitigation measures in terms of reduced mobility and teleworking and its joint effect on urban air pollution. As sharp drops in air pollution during confinement periods indicate, COVID-19 experiences may teach us some important lessons about how the deadly global air pollution crisis might be overcome. More than 80% of the people living in urban areas are exposed to air quality levels that do not meet air quality standards of the World Health Organization³, with populations in low-income cities being most impacted⁴. In the European Union (EU-28) it was estimated that long-term exposure to elevated Particulate Matter with a diameter of $\leq 2.5 \mu\text{m}$ (PM2.5) concentrations were responsible for about 374,000 premature deaths in 2016; exposure to enhanced nitrous oxide (NO_2) and ozone (O_3) levels led to $\sim 68,000$ and 14,000 additional premature deaths, respectively⁵. Moreover, the finding of some recent studies show that short-term and long-term exposure to air pollution, especially PM2.5 and NO_2 , contribute to aggravating COVID-19 infections and mortalities^{6–8}. Traffic emissions typically contribute 30–45% to urban air pollution⁹. Consequently, COVID-19 mitigation measures that included important reduction of traffic have

caused pollution levels to drop significantly. This was first observed in China, where satellite images of emissions showed a decrease of NO_2 emissions by 30%^{10,11}, and was later reported from many parts of the world^{12–15}. The European Environmental Agency has been tracking the weekly average concentrations of air pollutants (NO_2 , Particulate Matter with a diameter of $\leq 10 \mu\text{m}$ (PM10, PM2.5) of many European cities where restrictive measures have been implemented¹⁶, showing that most cities reduced contamination levels by 30–50% compared with the same period in 2019. In addition, estimated averaged emissions reduction in Europe during the COVID-19 lockdown were reported (-33% for nitrogen oxides (NO_x), -8% for non-methane volatile organic compounds, -7% for sulfur oxides (SO_x), and -7% for PM2.5) with an 85% contribution of the road transport to the total reductions except for SO_2 for which reductions were mainly driven by the energy and manufacturing industry sectors¹⁷. Overall, most of the studies show a correlation between the reduction in mobility data and trend of PM2.5 and NO_2 ^{17,18}. These observations prompt us to think that if we are able to enhance teleworking and reduce traffic emissions so drastically and promptly to stop the spread of the COVID-19 we are capable of taking similar measures to stop other deadly diseases related to the poor air-quality in cities. It seems timely to question whether we need to move back to the deadly 'pre-corona' configuration of urban traffic and emission patterns, and whether it would be possible to establish similar traffic restrictions as during the pandemic in order to reduce premature deaths from air pollution. It is important to reflect to which extent our commuting and travels really are essential, and to which extent we can implement teleworking to avoid traffic emissions, as evidenced during the confinement period.

A first observation from the large scale COVID-19 lockdown indicates that people in many sectors are capable of building up resilience to the limitation of traveling to work, and—despite

¹Sostenipra Research Group, Institute of Environmental Sciences and Technology, Universitat Autònoma de Barcelona, Barcelona, Spain. ²Barcelona Lab for Urban Environmental Justice and Sustainability (BCNUEJ), Urban Hospital del Mar Medical Research Institute (IMIM), Barcelona, Spain. ³Department of Geography, Humboldt Universität zu Berlin, Berlin, Germany. ⁴Solució de Ciutat i Territori d'Anthesis Lavola, Rambla Catalunya, 6, 2^a planta, Barcelona, Spain. ⁵PCOT Team, Institute Cartographic and Geological of Catalonia (ICGC), Barcelona, Spain. ⁶GAMA Team Department of Applied Physics, University of Barcelona (UB), Barcelona, Spain. ⁷Departament d'Arquitectura de Computadors i Sistemes Operatius (CAOS), Escola d'Enginyeria, Universitat Autònoma de Barcelona, Barcelona, Spain. ⁸Department of Chemical, Biological and Environmental Engineering, Universitat Autònoma de Barcelona, Barcelona, Spain. [✉]email: gara.villalba@uab.cat

indisputable frictions—adapt to new modes of work without the requirement of physical displacements, including both daily travels to work by car as well as air-bound travels¹⁹. During the lockdown, we could observe first-hand how the higher education sector has started to professionalize forms of online teaching²⁰, while scientific conferences are increasingly held virtually. Also, public administrations start to arrange new data management systems accessible remotely and many white-collar workers in industries and services are experiencing that they can fulfill most of their duties as well from their home-offices. Even medical doctors have started teleworking via telephone and internet-based consultancies²¹. Figures from Google (2020) observing mobility during the COVID-19 lockdown² indicate that the presence at work spaces dropped by over 60% in countries where strict lockdown measures enforced a maximum of teleworking, such as in Spain or Italy.

In the EU and overall global north, with over 70% of the people working in the service sector, we must start to question much stronger which parts of the usual level of daily displacements are really necessary. The current crisis is teaching us that for many people daily commuting is related to habits and traditions in organizing their work rather than to actual necessities and therefore a rethink of how to restructure work in a more air-pollution-efficient way is required. We should keep in mind that metropolis, which generate and attract a great number of motorized displacements, are currently the areas where the main air quality problems are happening²². Teleworking (not only avoiding commuting to and from home, but also replacing meetings with video calls) entails an important reduction of those emissions related to mobility^{23,24}. An extensive review of the energy impacts of teleworking by Hook et al.²⁴ summarizes that the energy savings from reduced commuter travel are greater than the indirect energy consumption associated with changes in non-work travel and home energy consumption. A study of Switzerland traffic congestion determined that teleworking was responsible for 1.9% reduction of the air pollution and concluded that teleworking is a promising tool for urban planning and development to reduce traffic volume and improve air quality²³. This study in particular shows that the largest changes in air pollutants concentrations due to teleworking are observed for NO₂ with a 3.6% reduction, followed by 3.4% for CO, 3.3% for PM and between 2.1 and 2.3% for O₃ and SO₂. Another study of a teleworking scenario in the United States shows that increased teleworking decreases CO₂ emissions by 2–80%, NO_x by 20–100%, PM₁₀ by 10–100%, and CO by 20–100%²⁵. Teleworking practices have been gaining momentum in digital-based jobs as a means to increase job satisfaction and productivity^{26,27} and are expected to experience rapid growth in the future²⁸.

We are at an important turning point in the conception of telework. The European Commission in a recent communication highlights the important role of telework in preserving jobs and production in the context of the Covid-19 crisis²⁹. The COVID pandemic has weakened some of the limiting factors of teleworking, and we can now conceive future socio-occupational scenarios in which telework is more recurrent. Among the factors that have previously limited a greater proliferation of telework, the most important are lack of specific regulations as well as lack of willingness by managers and workers alike. The crisis situation caused by the outbreak of COVID-19 has led many companies to use telework as an emergency solution, in order to be able to continue many non-essential productive activities¹⁹. Additionally, progress has been made on other aspects that were previously limiting, such as information and communication technologies to facilitate telework, and the transition to a more knowledge-intensive economy. COVID-19 has also encouraged online over face-to-face education, as well as a widespread reduction in personal mobility. For instance, according to the Labor Force Survey (EPA) of the National Statistics Institute (INE) of Spain,

during the second quarter of 2020, 16.20% of employed people worked from home for more than half of the days, compared to 4.81% observed in 2019³⁰. This comparison illustrates the potential of tele-workable jobs that were not previously run remotely.

In short, the exceptional situation during COVID-19 can be understood as a large-scale pilot test of the implementation of teleworking and related traffic reduction, in order to reduce air pollution levels in cities. The objective of this article is to further examine the potential of future socio-occupational scenarios in reducing air pollution in cities. We focus our analysis on NO₂ concentrations where we see the biggest changes due to teleworking. Variability in O₃ concentrations is also analyzed due to the role of NO_x in O₃ loss and production.

RESULTS

Study case

To discuss the wider implications of enhanced teleworking and targeted traffic restrictions to improve urban air quality in cities, we study the Metropolitan Area of Barcelona (AMB), Spain, during the strict confinement in spring 2020. The AMB has more than 5 million people and is the most populated urban area on the Mediterranean coast and one of the largest metropolis in Europe. Barcelona annually reports one of the highest air pollution levels Europe-wide³¹, with the most problematic pollutants being PM2.5, PM10, and NO₂^{31–33}. In particular, in 2019 the NO₂ annual mean exceeded the WHO guideline³ and the legal limit in the UE of 40 $\mu\text{g m}^{-3}$ in the urban air pollution ground monitoring stations representing high traffic (Eixample and Gràcia-Sant Gervasi). Also that year, the mean value for PM10 and PM2.5 was above the WHO guideline³ of 20 and 10 $\mu\text{g m}^{-3}$, respectively in all urban stations in the city³¹. In the city of Barcelona alone, the excess of air pollution beyond the recommended WHO guidelines was deemed responsible for 7% of natural mortalities (about 1000 annual deaths), 11% of new lung cancer cases and 33% of new childhood asthma cases in 2019³³. Road traffic is the main source of NO_x, responsible for 59% of all emissions in the AMB, while the seaport is the second largest emission source with 16%³⁴.

The complex topography of the AMB is characterized by inland mountain ranges (Fig. 1) protecting the area from Atlantic advections and continental air masses, but also blocking the dispersion of pollutants³⁵, while the valleys of the rivers Llobregat and Besòs play an important role in the creation of air-flow patterns³². Thus, the atmospheric flow at AMB is complicated not only by the urban heat island effects but also topographic flows and sea breezes which influence air pollution and human health.

As one of the countries hardest hit by COVID-19, the mobility restrictions during the COVID-19 lockdown in Spain² were among the strictest globally; only manufactory and warehouse workers, farmers, supermarket clerks and nursing staff were permitted to commute as they were deemed essential to maintain the core functions of the society, such as the provision of food, energy, health care, and internet among others. Maintaining these basic functions required about 36% of the displacements to workspaces compared to the pre-corona business-as-usual, according to the Google mobility reports for Catalonia for March 2020². Similar to other urban areas in Europe, the economy in the AMB is dominated by the tertiary sector (90.1% of salaried jobs and 88.3% of the self-employed) and showed a general potential to reduce traffic significantly without losing the maintenance of basic functions, at least for a short period of time.

COVID-19 mobility reduction and improved air quality

Observational data from various urban and suburban monitoring stations throughout the AMB (Fig. 1) indicate that the COVID-19 lockdown during March and April 2020 significantly reduced

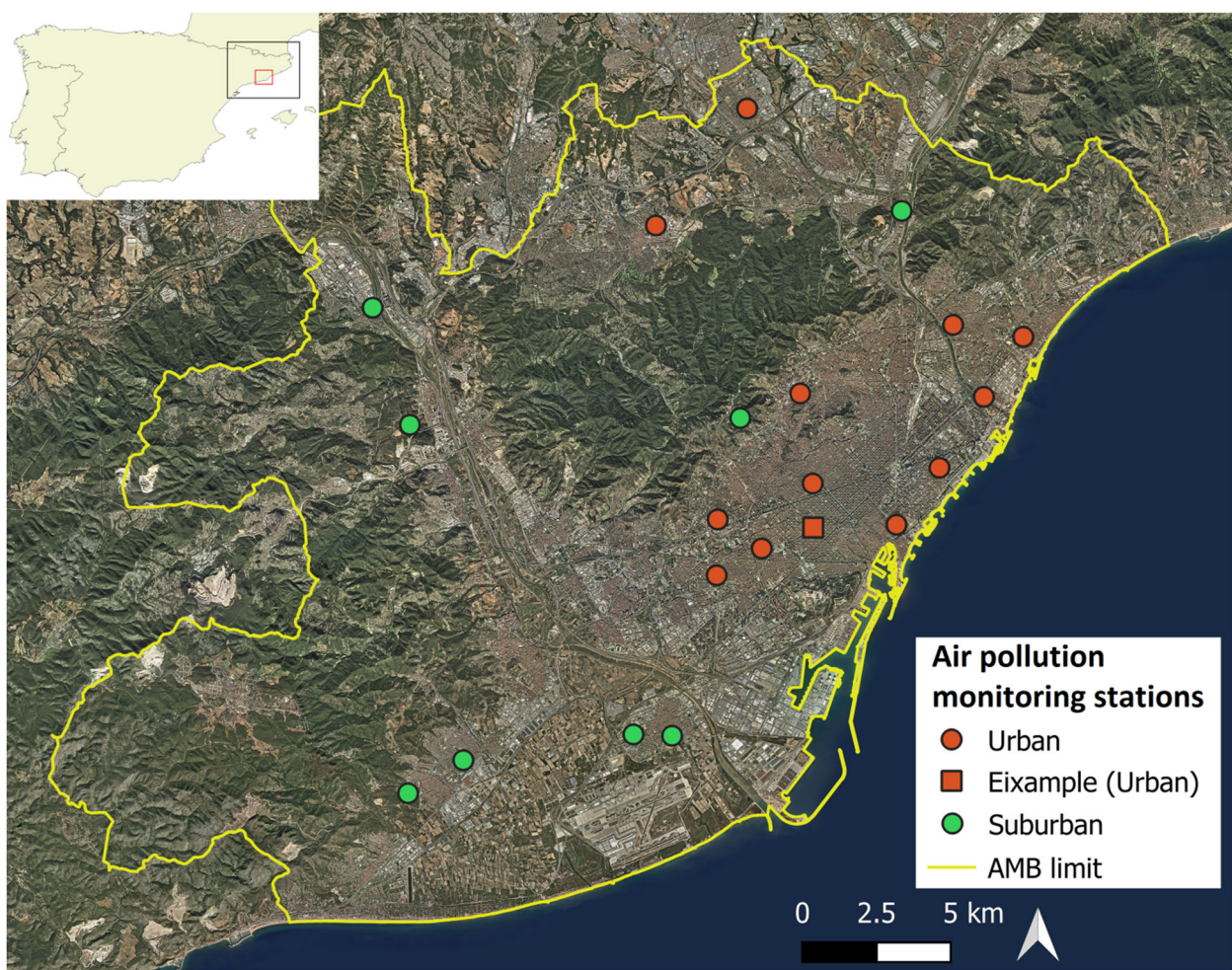


Fig. 1 **Metropolitan Area of Barcelona as a study case for air pollution reduction.** Smaller map: location of domain used for the simulation of regional chemistry transport model WRF-Chem (black frame), and the area of study the AMB (red frame). Larger map: a more detailed map of the AMB indicating the urban and suburban air pollution monitoring stations (Xarxa de Vigilància i Previsió de la Contaminació Atmosfèrica, XVPCA).

principal air pollutants, including NO_2 , PM_{10} and SO_2 ^{14,36}. We illustrate Monday–Friday hourly averages of NO_2 concentrations in Fig. 2 for 2020 (in blue) and 2019 (in orange) for the highly intense traffic area monitored by the *Eixample* air pollution station (red square in Fig. 1). These 2 years had similar stable surface pressures (1016 hPa in both cases), temperature anomalies (around 2 °C in 2019 and 2.5–3 °C in 2020), and low winds, albeit 2019 was a drier year (please refer to Supplementary Table 1 and Supplementary Table 2 for a detailed report of the meteorological conditions for the study period for both years). Just the same, to reduce the influence of the meteorological conditions on the comparison, the hourly averages presented for 2019 are calculated based on the entire month, rather than week by week as it is shown for 2020. Furthermore, we include a weekly estimation of the mobility reduction based on Google COVID-19 Community Mobility Reports². For example, the mobility reduction during the first and second week of the confinement, 75.4% and 82.2% respectively, caused a reduction of NO_2 concentration of 53% and 59%, respectively, compared to 2019. During the third week of the lockdown, with the highest mobility reduction (84.4%), NO_2 concentrations were observed to drop down to 21 $\mu\text{g m}^{-3}$ during morning peak hour, a 75% reduction when compared to March 2019. Reductions were especially distinctive during the typical daily pollution peaks around 8 and 21 h when the medians (50th

percentile) went down from values around 80–20 $\mu\text{g m}^{-3}$ (at 8 h), and from 65 to 10 $\mu\text{g m}^{-3}$ (at 21 h).

We also find that the low pressures and cyclonic weather associated to low pressures seen in weeks 3, 6, 7, 9, 12, 13 of 2020 (see Supplementary Table 1 for more information) enhance gas dispersion thereby reducing pollutant concentrations, while higher pressures have the opposite effect. This is clearly seen when comparing the third and fourth week of the lockdown with similar mobility reductions (84.4%), yet during the fourth week we can see higher NO_2 concentrations during morning peaks (from 18–20 to 55–57 $\mu\text{g m}^{-3}$). Hence, traffic reductions are not the only cause for lower air pollution levels during the COVID-19 lockdown, evidencing a significant role of the meteorological conditions in reducing the concentrations of air pollutants.

Unlike NO_2 , Ozone (O_3) levels increased during the period of confinement in the AMB. During the fourth week of the lockdown we can observe the most pronounced O_3 peak at 16 h with a median value of 150 $\mu\text{g m}^{-3}$, approximately double that of April 2019. The remaining weeks the ozone values are also clearly higher than in 2019. Ozone is not reduced as the other pollutants as a consequence of three combined effects^{37,38}: (1) decrease of NO_x in a volatile organic compounds (VOCs)-limited (low VOC/NO_x ratios) urban environment might cause O_3 to increase, as opposed to the behavior at the rural-regional background, which is mainly NO_x -limited (high VOC/NO_x ratios); (2) reducing nitrogen oxide

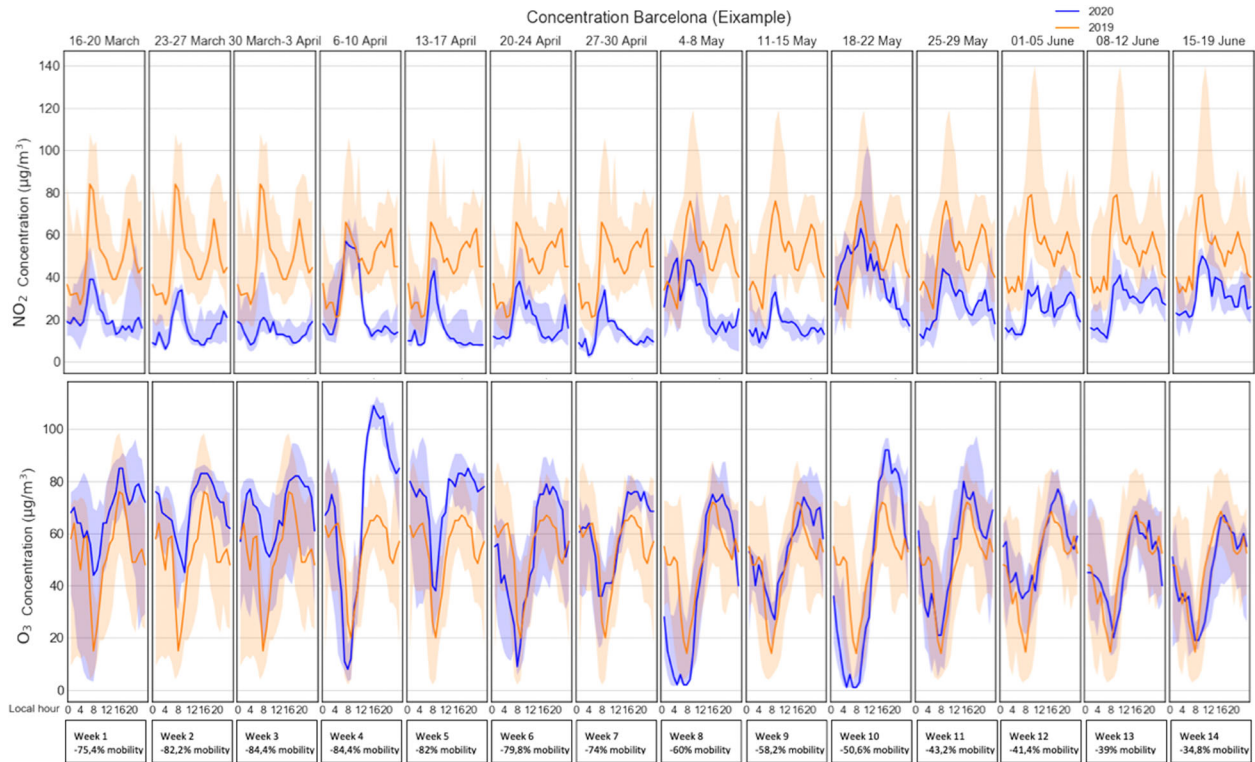


Fig. 2 NO₂ and O₃ concentration during COVID-19 mobility restrictions. Variation for NO₂ and O₃ concentrations during COVID-19 confinement and phase-out weeks (in blue) and the same month for the year 2019 (orange), observed at Eixample air quality monitoring station (as part of the Xarxa de Vigilància i Previsió de la Contaminació Atmosfèrica, XVPAC). Blue and orange lines show the medians (50th percentile) and shaded zones show the 10th/90th percentiles. An estimation of the reduction in travel by vehicle during 2020 is provided underneath each panel, source: Google mobility reports (<https://www.google.com/covid19/mobility/>).

(NO) levels slows down the ozone (O₃) consumption (titration of O₃, NO + O₃ = NO₂ + O₂) and causes an increase of O₃ concentrations; and (3) the usual increase of insolation and temperatures from February to April leads to an increase in O₃.

Consequently, O₃ concentrations during lockdown exceeded the maximum value established by the WHO, which is 100 µg m⁻³ averaged over an 8-h period. This enhancement of O₃ was also found in other cities during the COVID-19-related mobility restrictions^{10,14,39}. Overall, however, the observations evidence a significant improvement of the air quality due to the restrictive mobility measures¹⁴. For a more detailed description of air quality during the confinement and de-confinement phases of COVID-19 for Barcelona, please visit www.urbag.eu/news/.

Air pollution modeling

The simulation of the base scenario March 2016 using HERMESv3 shows that the highest NO emission peaks occur in the central parts of the AMB during the morning and afternoon (as can be appreciated in Fig. 3B, C, E, F), due to the high concentration of traffic throughout the day. Once NO is emitted, it is rapidly converted to NO₂ in the presence of O₃ through oxidation reactions that take place in less than the tenths of seconds^{37,38}. This conversion depends on the concentration of O₃ and VOCs, solar energy, and meteorological conditions^{37,38}. The WRF-Chem simulations indicate that the highest NO₂ concentrations are observed in the north of the AMB (Fig. 3A, D) due to the combination of the atmospheric northward plume characteristic of this area and the complex topography (Fig. 1) that pulls the pollutants towards the north of the AMB during both morning and evening peaks.

The simulation of the base case scenario has been evaluated with several air quality monitoring stations (that belong to the

monitoring network: Xarxa de Vigilància i Previsió de la Contaminació Atmosfèrica, XVPAC) over the AMB for NO₂ and O₃ (see Supplementary Figs. 1 and 2). Overall, the model shows a reasonable agreement with the observations during the period of March, although there are specific periods showing significant biases (−35 and 26 µg m⁻³, for NO₂ and O₃, respectively) over the urban stations representing high traffic (Eixample, Gràcia-Sant Gervasi and Poblenou). However, the model exhibits low biases (−20 and 12 µg m⁻³, for NO₂ and O₃, respectively) at stations located in a low traffic area (Ciutadella, Vall d'Hebron, Palau Reial and Sants) for specific periods. Surface NO₂ and O₃ concentrations are very sensitive to the emissions, therefore, these model biases are mostly due to the low resolution in our emission inventory.

Based on the perturbed emissions simulations, we estimate that city-wide NO₂ concentrations during a severe lockdown scenario are reduced by as much as 52% (22 µg m⁻³) during the typical morning high pollution peak between 7 and 9 h, as shown in Fig. 4 (and in Supplementary Fig. 3), comparable to the observations during the COVID-19 lockdown (weeks 1–7 in Fig. 2). Similarly, the medium confinement scenario reduces NO₂ concentrations by 33% (13 µg m⁻³), comparable to weeks 8 through 10 (Fig. 2). As was observed during the fourth week of confinement, reductions of NO_x emissions alleviate the effect of ozone titration^{37,38} leading to a significant increase in O₃ concentrations for the lockdown scenario up to 61% (18 µg m⁻³) and under the medium confinement scenario up to 35% (11 µg m⁻³) (see Supplementary Figs. 4 and 5). In some areas of the AMB, these extreme mobility reduction scenarios are thus partly counterproductive in terms of alleviating air pollution, since O₃ levels exceed the daily maximum 8-h mean of 100 µg m⁻³. On the contrary, the low confinement scenario results in 16% reduction of NO₂ concentrations (−6 µg m⁻³) and an increase of O₃ concentrations (+5 µg m⁻³). Although we cannot make a direct correlation between emission reduction

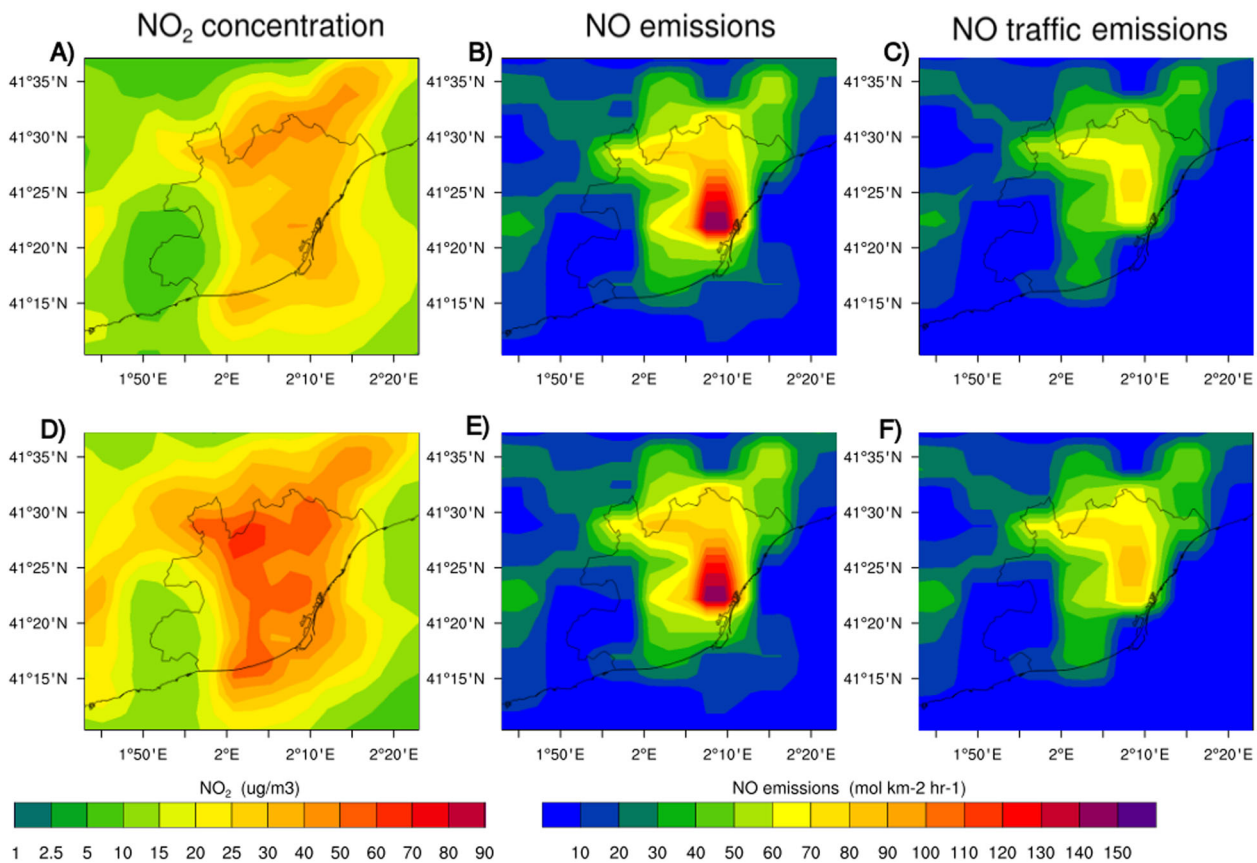


Fig. 3 NO₂ pollution peaks in the Metropolitan Area of Barcelona (AMB). Average NO₂ concentrations (A, D), NO total (B, E) and traffic emissions (C, F) for the base scenario during morning (top panels) and afternoon (bottom panels) peaks time for March 2016 (only weekdays Monday–Friday). The peak time for the concentrations is 7–9 h (morning) and 21–23 h (afternoon). The peak time for the emissions is 6–8 h (morning) and 15–17 h (afternoon).

and resulting pollutant concentrations because atmospheric chemistry is not only influenced by changes in emissions but also by atmospheric dynamics such as transport, we can infer some conclusions based on the simulations. Results show that by intensifying teleworking efforts to 2 and 3 days a week, NO₂ concentrations are reduced, averaging reductions over the entire AMB of 4% ($-1.5 \mu\text{g m}^{-3}$) and 8% ($-3 \mu\text{g m}^{-3}$) in the low and moderate increase telework scenarios, respectively. We also find that during high pollution episodes air quality over all the AMB region improves by changing from 2 days per week telework (low-increase telework scenario) to 4 days a week (high-increase telework scenario) with an overall 10% reduction ($-6 \mu\text{g m}^{-3}$) and a slight increase of up to $3 \mu\text{g m}^{-3}$ of O₃ concentrations.

Similar results are seen during the typical evening high pollution peaks between 21 and 23 h shown in Fig. 5 (and in Supplementary Fig. 6), where a full lockdown scenario reduces the NO₂ concentrations by as much as 53% ($-27 \mu\text{g m}^{-3}$) and increases O₃ by 70% ($+25 \mu\text{g m}^{-3}$), see Supplementary Figs. 7 and 8 comparable to the observed concentrations during weeks 1 through 7 (Fig. 2). The medium confinement scenario simulation shows NO₂ concentration reduction of 35% ($-17 \mu\text{g m}^{-3}$) similar to weeks 8, 9, and 10 of the confinement periods (Fig. 2). The low confinement scenario results in 13% reduction of NO₂ concentrations and an increase of O₃ concentrations (up to $8 \mu\text{g m}^{-3}$). Note that there is a slight increase in NO₂ ($1 \mu\text{g m}^{-3}$) and decrease of O₃ ($1 \mu\text{g m}^{-3}$) for the moderate and low telework scenarios around the harbor area that could be related to local O₃–NO_x changes in reducing traffic emissions. In general, reductions for all scenarios are seen over all the territory with higher reductions located on

the north of the AMB where higher pollution is found during the day (see Fig. 3).

In short, teleworking can be a key tool in alleviating traffic congestion during peak time and improve air quality in a short term (days–weeks) particularly in the urban areas, where high population density and the hotspots for traffic emissions are found.

DISCUSSION

Mobility restrictions implemented worldwide to contain and delay the spread of the COVID-19 epidemic have drastically reduced traffic² and corresponding emissions, and effected on reducing air pollution levels^{10–15,36}. In particular, we observe that NO₂ concentration values in the city of Barcelona during COVID-19 mobility restrictions were below the WHO thresholds which had been exceeded at several urban air pollution monitoring stations during the same period in previous years³¹. The COVID-19 inspired modeling efforts to indicate that air pollution reduction might be reached relatively easily through enhanced teleworking. Although these figures are still premature, and a more in-depth investigation is required as to whether productivity standards can be maintained under teleworking conditions and whether other environmental costs emerge (e.g. less efficient use of space and other resources, doubling of equipment etc.), urban policy makers should question how they can better target their instruments, and which incentives they can provide and which restrictions can be implemented to maintain some of the positive effects on air pollution we are seeing during COVID-19. This might include more flexible work schedules, starting with the public administration,

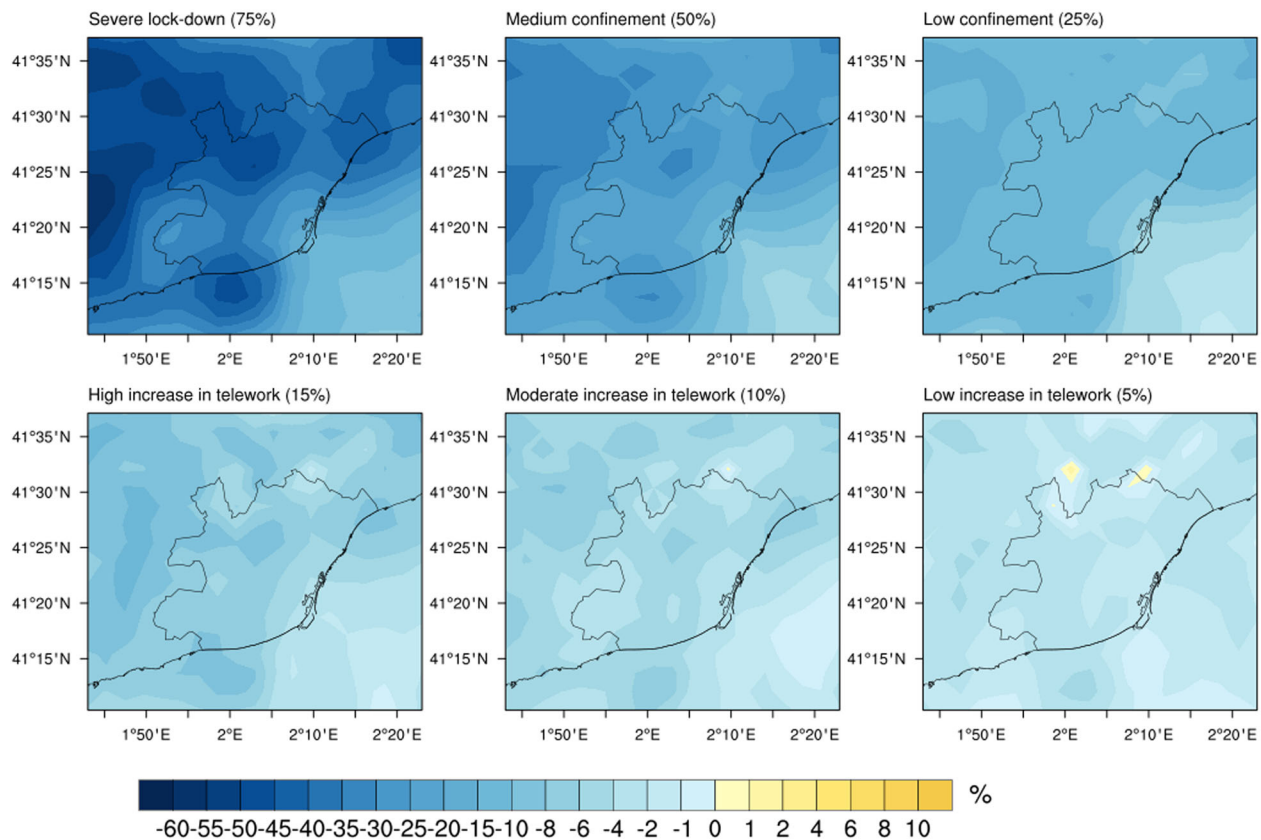


Fig. 4 NO₂ concentration differences during morning peak hours. Difference (in %) in NO₂ concentrations between the base case and each scenario during typical morning high pollution peak hours (7–9 h) in the Metropolitan Area of Barcelona for March 2016 (only weekdays days Monday–Friday).

possibly tax advantages for home offices to lower the general emission level, up to targeted traffic restrictions for low priority travels when threshold levels for air pollution are surpassed. The COVID-19 lockdown observations and our corresponding simulation indicate that a 25% emission reduction scenario during periods of high pollution is achievable, simply based on the maximization of teleworking and reducing other work-related travel and shopping. To the contrary, stronger traffic reductions related to 50 and 75% emission reduction scenarios seem to embed an unintended feedback manifested in an increase of O₃ concentrations, and thus not seem to be appropriate measures.

Our study provides the empirical and modeled evidence to intensively promote teleworking as a means to lower urban pollution levels. Annual average NO₂ concentrations have repeatedly exceeded maximum permissible values over the last 5 years in some stations of the AMB, consequently causing thousands of premature deaths^{34,40}. Results show that by intensifying teleworking efforts to 2, 3, and 4 days a week, NO₂ concentrations are reduced, averaging reductions over the entire AMB during the day of 4% ($-1.5 \mu\text{g m}^{-3}$), 8% ($-3 \mu\text{g m}^{-3}$), and 10% reduction ($-6 \mu\text{g m}^{-3}$). Indeed, teleworking can be an effective solution to reduce traffic and improve air quality, which can be implemented immediately leveraging on our experience during the COVID-19 mobility restrictions and in addition to other mitigation strategies such as Low Emissions Zones (LEZ). Unlike LEZs, teleworking can be implemented much more rapidly and furthermore reduces the amount of fossil fuel consumed and consequently the carbon footprint of the city.

The COVID-19 period has shown that in general higher-paid jobs have higher adaptive capacities for teleworking. This means mandatory teleworking will more strongly affect well-paid white-collar workers. While other instruments to lower emissions, such as

bans of older cars as imposed by LEZ as well as fuel tax reforms tend to discriminate those with lower income⁴¹. Emission reductions based on mandatory teleworking might be socially more equal and partly compensate for unequal emission patterns among different social groups, for example, in relation to leisure-related travels. Apart from that, teleworking allows for flexible schedules and a greater work-life balance while reducing the mobility. Therefore, teleworking might also reduce the amount of accidents a (both *in itinere* and *in labore*)^{42,43} and lower other economic, social and environmental costs linked to the current mobility model⁴⁴. Besides, the Covid-19 crisis shows us how teleworking has been used by companies to provide a safe and healthy working environment to their employees' and the continuity to economic activity¹⁹.

In short, COVID-19 has opened an important opportunity to rethink more radically, measures and opportunities to combat the urban air pollution crisis we are facing in cities. Policies that steer people's mobility by enhancing teleworking might not only be efficient in decreasing emissions and easily implemented, but are also likely to be more socially equitable than other measures primarily used for this purpose until today.

METHODS

Future socio-occupational scenarios

In order to understand the effect of mobility on air quality during the lockdown and to explore the potential of teleworking towards air pollution reduction, we define six scenarios with traffic emission reductions resulting from various degrees of teleworking and reduced private vehicle use. Based on the justified estimates that 85% of the labor force of the AMB is dedicated to the service sector⁴⁵, and that ~40% of all personal vehicle

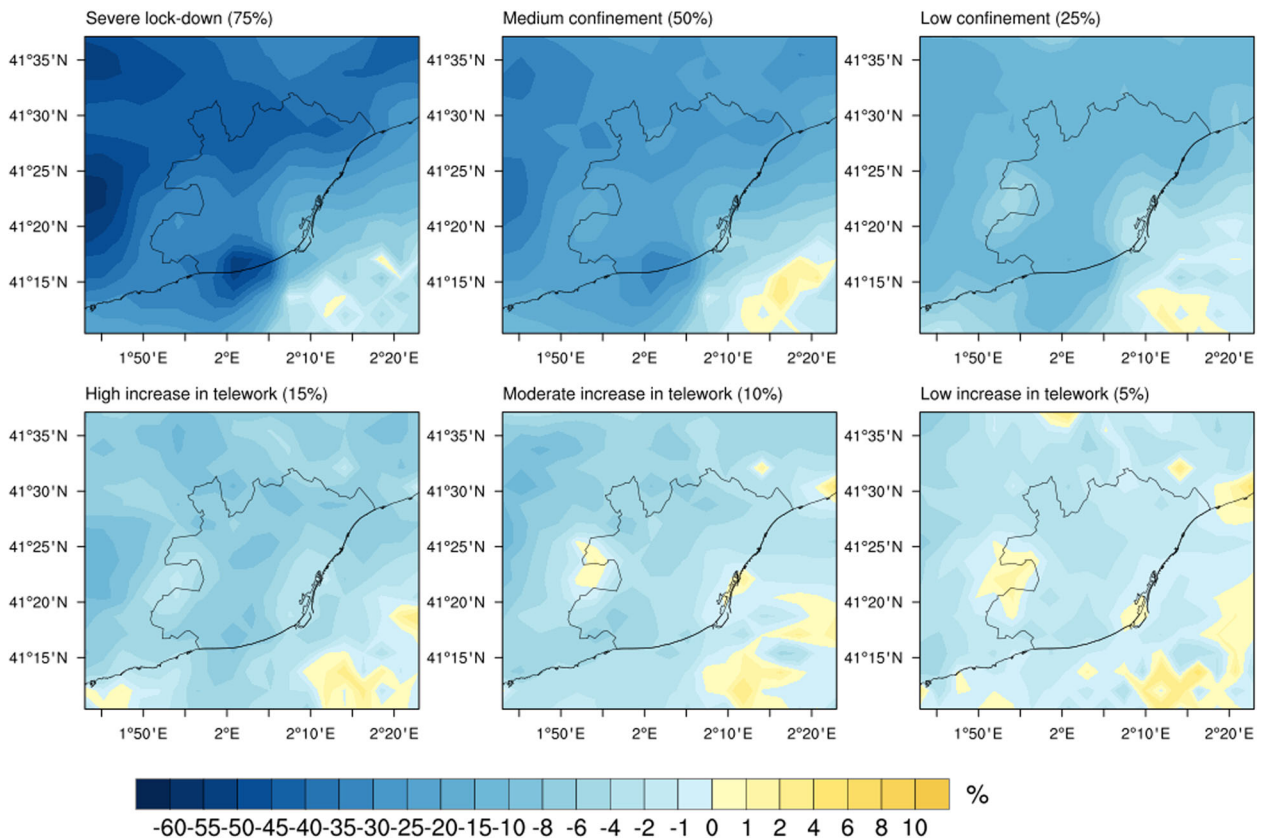


Fig. 5 NO₂ concentration differences during evening peak hours. Difference (in %) in NO₂ concentrations between the base case and each scenario during typical evening high pollution peak hours (21–23 h) in the Metropolitan Area of Barcelona for March 2016 (only weekdays Monday–Friday).

transit is work-related⁴⁶, we define the following three scenarios of enhanced telework:

- (1) Low increase in telework = 5% traffic emission reduction: Requires 7.5–12.5% decrease in work-related traffic, obtained by 20% of the labor force of the service sector adopting teleworking 2 days a week, resulting in an overall 5% reduction of traffic-related emissions (40% × 0.20 × 2/5).
- (2) Moderate increase in telework = 10% traffic emission reduction: Requires 17.5–25% decrease in work-related traffic; obtained by 30% of the labor force of the service sector teleworking 3 days a week, resulting in an overall 7.2% reduction of traffic-related emissions (40% × 0.30 × 3/5 and rounded up to 10% to account for additional work-related trips that are avoided during teleworking days).
- (3) High increase in telework = 15% traffic emission reduction: Requires 32.5–37.5% decrease in work-related traffic; obtained by 40% of the labor force of the service sector teleworking 4 days a week, resulting in an overall 12.8% reduction of traffic-related emissions (40% × 0.40 × 4/5 and rounded up to 15% to account for additional work-related trips that are avoided during teleworking days).

Moreover, we define three additional scenarios combining reduction of personal and occupational mobility in addition to teleworking, to replicate behaviors seen during the main COVID-19 confinement stages of severe lockdown (March 16th–April 30th, see Fig. 1 weeks one through seven), medium confinement (May 1st–June 12th, see Fig. 1 weeks 8 through 13), and low confinement (June 12th onwards, see Fig. 1 week 14). All calculations are made based on the mobility report published by Autoritat del Transport Metropolità de l'Àrea de Barcelona⁴⁷.

- (4) Low confinement = 25% traffic emission reduction: Resulting from 45% reduction of private vehicle use for work-related travel (accomplished by teleworking 4 days a week and reducing other work-related vehicle activity by 15%). Additionally, online education avoids 20% of private vehicle use, and people reduce driving for shopping by 30%. No reductions are in effect for leisure and personal travel.

- (5) Medium confinement = 50% traffic emission reduction: Resulting from 55% reduction of private vehicle use for work-related travel (accomplished by teleworking 4 days a week and reducing other work-related vehicle activity by 20%). Additionally, online education avoids 20% of private vehicle use, and people reduce driving for shopping by 40%. Vehicle use related to personal activities such as leisure, accompaniment, and health-related appointments are all reduced between 50 and 70%.
- (6) Severe lockdown = 75% emission reduction: Resulting from 55% reduction of private vehicle use for work-related travel (accomplished by teleworking 4 days a week and reducing other work-related vehicle activity by 20%). Additionally, online education avoids 100% of private vehicle use, and people reduce driving for shopping by 70%. Vehicle use related to personal activities such as leisure, accompaniment, and health-related appointments are all reduced between 75 and 100%. This scenario seems only feasible during short periods of time and during absolute extreme situations. This simulation serves as a comparison of model simulation with observations.

Telework also allows business meetings to be conducted remotely without the taking long business trips by airplane. In order to represent in a simple way these remotely business trips, air traffic has also been reduced in each scenario with the same reduction as road traffic.

Air quality modeling

The regional chemistry transport model WRF-Chem⁴⁸ version 4.1, a highly flexible community model for atmospheric research where aerosol–radiation–cloud feedback processes are taken into account, is used in this study. The WRF-Chem model has been previously used for simulations of air pollution episodes^{49–51}. For the gas-phase chemical scheme, we used the Regional Acid Deposition Model (RADM2⁵²) and the MADE/SORGAM aerosol scheme^{53,54}. RADM2 has been broadly used in air quality studies over Europe^{55,56}. The model is set up with a horizontal resolution of 3 × 3 km and 45 vertical layers up to 100 hPa. The meteorological initial and lateral

Table 1. Model details and experiment configuration.

Model details	
Gas-phase scheme	RADM2 ⁵²
Aerosol particles	MADE/SORGAM ^{53,54}
Photolysis scheme	FAST-J ⁷¹
Urban scheme	BEP + BEM ⁵⁹
Biogenic emissions	MEGANv2 ⁶⁵
Experiment configuration	
Horizontal resolution	3 × 3 km
Vertical layers	45, up to 100 hPa
Chemical initial condition	MOZART-4 ⁵⁸
Meteorological initial condition	FNL-NCEP ⁵⁷
Chemistry spin-up	1 month
Emission inventories	CAMS-REG-APv3.1 ⁶³

boundary conditions were determined using the Final Analysis (FNL) of the NCEP global model data⁵⁷. Chemical initial and boundary conditions are from the global atmospheric model MOZART-4 global chemical model⁵⁸. We conducted WRF-Chem simulations for March 2016 covering the Catalonia domain (see boundaries in Fig. 1) with a spin-up of 1 month. In order to represent the urban areas in our domain, here we used a multi-layer urban canopy scheme, the Building Effect Parameterization (BEP) coupled with the Building Energy Model (BEP + BEM⁵⁹) that takes into account the energy consumption of buildings and anthropogenic heat, which has been previously validated for the area under study⁶⁰. The Local Climate Zones (LCZ) classification⁶¹ is used for the AMB which associates a specific value for each LCZ for thermal, radiative and geometric parameters of the buildings and ground, which are used by the BEP + BEM urban canopy scheme to compute the heat and momentum fluxes in the urban areas. Eleven LCZs with specific urban morphology for each were added into the land-cover map.

The HERMESv3 preprocessor tool⁶² was used in order to create the anthropogenic emissions files from the CAMS-REG-APv3.1 database⁶³. Biogenic emissions are computed online from the Model of Emissions of Gases and Aerosols from Nature v2 (MEGAN⁶⁴). Six air quality simulations are performed under each emission scenario (75, 50, 25, 15, 10, and 5% reduction on traffic emissions) and compared with the base case scenario simulation (no reduction in traffic emissions) for the period of March 2016 to study the impact of the lockdown measures on air quality and how teleworking can improve the air pollution over the AMB. Simulations are based on data from 2016, the most recent year for which emission inventories are readily available. According to the meteorological data from the Servei Meteorològic de Catalunya^{65,66}, the average surface pressure was 1014.5 hPa for 2016 and 1016 hPa for 2020, the wind intensity was low/moderate around 40 km/h (small trees in leaf begin to sway) for both periods, the temperature was 2.5–3 °C higher in 2020 and there was positive anomaly precipitation for both periods. Therefore, the simulations considered a similar period as the COVID-19 confinement (16th March until 30th April) in terms of climate, atmospheric stability, and synoptic conditions. Table 1 describes the main configuration of the model and experiment configuration.

DATA AVAILABILITY

The data generated and analysed during this study are described in the following data record: <https://doi.org/10.6084/m9.figshare.14743797>⁶⁷. The data from Xarxa de Vigilància i Previsió de la Contaminació Atmosfèrica (XVPCA), underlying Figs. 1–2 and Supplementary Figs 1–2, are openly available from Departament d’Acció Climàtica, Alimentació i Agenda Rural: http://mediambient.gencat.cat/ca/05_ambits_dactuacio/atmosfera/qualitat_de_laire/vols-saber-que-respires/descarrega-de-dades/descarrega-dades-automatiques/ (last access 6 June 2021). The CAMS emission data are available from Emissions of atmospheric Compounds and Compilation of Ancillary Data (ECCAD) at <https://doi.org/10.24380/m89g-j508>⁶⁸. The FNL-NCEP global model data are available from the National Center for Atmospheric Research (NCAR) Research Data Archive at <https://doi.org/10.5065/978H-D239>⁶⁹. The MOZART-4 global data are hosted by the NCAR and are available upon request via

the form at <https://www.acom.ucar.edu/wrf-chem/mozart.shtml> (last access: 5 March 2020). The WRF-Chem simulation outputs, underlying Figs. 4–5 and Supplementary Figs. 1–8, are openly available via the Zenodo repository at <https://doi.org/10.5281/zenodo.4767308>⁷⁰. The WMS maps underlying Fig. 1 are available in GIS format via the Cartographic and Geological Institute of Catalonia at: <https://www.icgc.cat/ca/Administracio-i-empresa/Serveis/Geoinformacio-en-linia-Geoserveis/WMS-i-tessel-les-Cartografia-de-referencia/WMS-Mapes-i-ortofotos-vigents>. The Butlletí climàtic mensual, supporting Supplementary Tables 1 and 2, is openly available from meteo.cat | Servei Meteorològic de Catalunya: <https://www.meteo.cat/wpweb/climatologia/el-clima-ara/butlleti-mensual/>. The April 2019 and April 2020 versions were used in the study.

CODE AVAILABILITY

The WRF-Chem model code is available from <https://www2.mmm.ucar.edu/wrf/users/downloads.html> (last access: 13 November 2020), with the specific code used in this study available from the authors upon request (Gara.Villalba@uab.cat). The HERMESv3.GR model code is available from https://earth.bsc.es/gitlab/es/hermesv3_gr.

Received: 28 October 2020; Accepted: 1 July 2021;

Published online: 17 August 2021

REFERENCES

1. Wang, C., Horby, P. W., Hayden, F. G. & Gao, G. F. A novel coronavirus outbreak of global health concern. *Lancet* **395**, 470–473 (2020).
2. Google L. L. C. COVID-19 Community Mobility Reports. <https://www.google.com/covid19/mobility/> (2020).
3. World Health Organization. Regional Office for Europe. *Air quality guidelines global update 2005: particulate matter, ozone, nitrogen dioxide and sulfur dioxide*. Copenhagen: WHO Regional Office for Europe. <https://apps.who.int/iris/handle/10665/107823> (2006).
4. World Health Organization. Air pollution levels rising in many of the world’s poorest cities. <https://www.who.int/news-room/12-05-2016-air-pollution-levels-rising-in-many-of-the-world-s-poorest-cities> (2016).
5. European Environmental Agency. Air quality in Europe—2019 report. No 10/2019. <https://doi.org/10.2800/822355> <https://www.eea.europa.eu/publications/air-quality-in-europe-2019/air-quality-in-europe-2019/viewfile#pdfjs.action=download> (2019).
6. Gupta, A. et al. Air pollution aggravating COVID-19 lethality? Exploration in Asian cities using statistical models. *Environ Dev Sustain* **23**, 6408–6417 (2021).
7. Ali, N. & Islam, F. The Effects of Air Pollution on COVID-19 Infection and Mortality —A Review on Recent Evidence. *Frontiers in Public Health* **8**, 580057 (2020).
8. Pozzer, A. et al. Regional and global contributions of air pollution to risk of death from COVID-19. *Cardiovasc. Res.* **116**, 2247–2253 (2020).
9. Trombetti, M. et al. Spatial inter-comparison of Top-down emission inventories in European urban areas. *Atmos. Environ.* **173**, 142–156 (2018).
10. Le, T. et al. Unexpected air pollution with marked emission reductions during the COVID-19 outbreak in China. *Science* **369**, 702–706 (2020).
11. Muhammad, S., Long, X. & Salman, M. COVID-19 pandemic and environmental pollution: a blessing in disguise? *Sci. Total Environ.* **728**, 138820 (2020).
12. Berman, J. D. & Ebisu, K. Changes in U.S. air pollution during the COVID-19 pandemic. *Sci. Total Environ.* **739**, 139864 (2020).
13. Sharma, S. et al. Effect of restricted emissions during COVID-19 on air quality in India. *Sci. Total Environ.* **728**, 138878 (2020).
14. Tobias, A. et al. Changes in air quality during the lockdown in Barcelona (Spain) one month into the SARS-CoV-2 epidemic. *Sci. Total Environ.* **726**, 138540 (2020).
15. Gautam, S. The Influence of COVID-19 on Air Quality in India: A Boon or Inutile. *Bulletin of Environ. Contam. Toxicol.* **104**, 724–726 (2020).
16. European Environmental Agency. Monitoring Covid-19 impacts on air pollution. <https://www.eea.europa.eu/themes/air/air-quality-and-covid19/monitoring-covid-19-impacts-on>
17. Guevara, M. et al. Time-resolved emission reductions for atmospheric chemistry modelling in Europe during the COVID-19 lockdowns. *Atmos. Chem. Phys.* **21**, 773–797 (2021).
18. Li, J. & Tartarini, F. Changes in Air Quality during the COVID-19 Lockdown in Singapore and Associations with Human Mobility Trends. *Aerosol Air Qual. Res.* **20**, 1748–1758 (2020).
19. Belzunce-Eraso, A. & Erro-Garcés, A. Teleworking in the Context of the Covid-19 Crisis. *Sustainability* **12**, 3662 (2020).
20. Mishra, L., Gupta, T. & Shree, A. OnlineTeaching-Learning in Higher Education during Lockdown Period of COVID-19 Pandemic. *Int. J. Educ. Res.* **1**, 100012 (2020).

21. Webster, P. Virtual health care in the era of COVID-19. *The Lancet* **395**, 1180–1181 (2020).

22. World Health Organization. Health as the pulse of the new urban agenda: United Nations conference on housing and sustainable urban development, Quito, October 2016. World Health Organization. <https://apps.who.int/iris/handle/10665/250367> (2016).

23. Giovanis, E. The relationship between teleworking, traffic and air pollution. *Atmos. Pollut. Res* **9**, 1–14 (2018).

24. Hook, A., Court, V., Sovacool, B. K. & Sorrell, S. A systematic review of the energy and climate impacts of teleworking. *Environ. Res. Lett.* **15**, 093003 (2020).

25. Kitou, E. & Horvath, A. Energy-related emissions from telework. *Environ. Sci. Technol.* **37**, 3467–3475 (2003).

26. Coenen, M. & Kok, R. A. W. Workplace flexibility and new product development performance: the role of telework and flexible work schedules. *Eur. Manag. J* **32**, 564–576 (2014).

27. Visser, J. & Ramos Martin, N. Expert Report on the Implementation of the Social Partner's Framework Agreement on Telework. <http://www.uva-aias.net> (2008).

28. Cegarra-Leiva, D., Sánchez-Vidal, M. E. & Cegarra-Navarro, J. C. Work Life Balance and the Retention of Managers in Spanish SME's. *Int. J. Hum. Res. Manag.* **23**, 91–108 (2012).

29. European Semester: Commission Communication on Country Specific Recommendations. https://ec.europa.eu/info/publications/2020-european-semester-commission-communication-country-specific-recommendations_en (2020).

30. National Statistics Institute of Spain. Labour Force Survey; 2nd Quarter 2020. https://www.ine.es/CDINEbase/consultar.do?mes=&operacion=EPA.%20Resultados%20trimestrales&id_oper=lr&L=1 (2020).

31. Rico, M. et al. Informe qualitat de l'aire de Barcelona, Technical report. *Agència de Salut Pública de Barcelona*. (2019).

32. Massagué, J. et al. 2005–2017 ozone trends and potential benefits of local measures as deduced from air quality measurements in the north of the Barcelona metropolitan area. *Atmos. Chem. Phys.* **19**, 7445–7465 (2019).

33. Rivas, I. et al. Child exposure to indoor and outdoor air pollutants in schools in Barcelona, Spain. *Environ. Int.* **69**, 200–212 (2014).

34. Schembri, A. et al. Traffic-related air pollution and congenital anomalies in Barcelona. *Environ. Health Perspect.* **122**, 317–323 (2014).

35. Soriano, C., Baldasano, J. M., Buttler, W. T. et al. Circulatory Patterns of Air Pollutants within the Barcelona Air Basin in a Summertime situation: Lidar and Numerical Approaches. *Boundary-Layer Meteorology* **98**, 33–55. <https://doi.org/10.1023/A:1018726923826> (2001).

36. Baldasano, J. M. COVID-19 lockdown effects on air quality by NO₂ in the cities of Barcelona and Madrid (Spain). *Sci. Total Environ.* **741** (2020).

37. Sillman, S. The relation between ozone, NO_x and hydrocarbons in urban and polluted rural environments. *Atmos. Environ.* **33**, 1821–1845 (1999).

38. Monks, P. S. et al. Tropospheric ozone and its precursors from the urban to the global scale from air quality to short-lived climate forcer. *Atmos. Chem. Phys.* **15**, 8889–8973 (2015).

39. Sicard, P. Amplified ozone pollution in cities during the COVID-19 lockdown. *Sci. Total Environ.* **735**, 139542 (2020).

40. Nieuwenhuijsen, M. J. et al. Air pollution, noise, blue space, and green space and premature mortality in Barcelona: a mega cohort. *Int. J. Environ. Res. Public Health.* **15**, 2405 (2018).

41. Zimmer, A. & Koch, N. Fuel consumption dynamics in Europe: Tax reform implications for air pollution and carbon emissions. *Transp. Res. Part A: Policy and Practice* **106**, 22–50 (2017).

42. Metropolitan Transport Authority. Mobility Strategy of the Metropolitan Transport Authority, Àrea de Barcelona. https://doc.atm.cat/ca/_dir_pde/20190404_Estrategia_Mobilitat_ATM.pdf (2019).

43. Dima, A.-M., Tuclea, C.-E., Vrânceanu, D.-M. & Tigu, G. Sustainable Social and Individual Implications of Telework: A New Insight into the Romanian Labor Market. *Sustainability* **11**, 3506 (2019).

44. Botzoris, G. N., Profillidis, V. A. & Galanis, A. T. Teleworking and Sustainable Transportation in the Era of Economic Crisis. *Proceedings of the 5th International Virtual Scientific Conference*. <https://doi.org/10.18638/ictic.2016.5.1.295> (2016).

45. Indicadors de la Unió Europea, Institut d'Estadística de Catalunya. www.idescat.cat/indicadors/?id=ue&n=10110 (2019).

46. Enquesta de mobilitat en dia feiner 2019 (EMEF). https://observatori.atm.cat/enquestes-de-mobilitat/Enquestes_ambit_ATM/EMEF/2019/EMEF_2019_Informe_AMB.pdf (2019).

47. Autoritat del Transport Metropolità de l'àrea de Barcelona, Observatori de la Mobilitat, Enquestes de mobilitat. <https://www.atm.cat/web/ca/observatori/enquestes-de-mobilitat.php>

48. Grell, G. A. Fully coupled “online” chemistry within the WRF model. *Atmos. Environ.* **39**, 6957–6975 (2005).

49. Georgiou, G. K. Air quality modelling in the summer over the eastern Mediterranean using WRF-Chem: chemistry and aerosol mechanism intercomparison. *Atmos. Chem. Phys.* **18**, 1555–1571 (2018).

50. Yegorova, E. A. Characterization of an eastern U.S. severe air pollution episode using WRF/Chem. *J. Geophys. Res.* **116**, D17306 (2011).

51. Shrivastava, M. et al. Modeling organic aerosols in a megacity: comparison of simple and complex representations of the volatility basis set approach. *Atmos. Chem. Phys.* **11**, 6639–6662 (2011).

52. Stockwell, W. R., Middleton, P., Chang, J. S. & Tang, X. The second generation regional Acid Deposition Model chemical mechanism for regional air quality modeling. *J. Geophys. Res.* **95**, 16343–16367 (1990).

53. Ackermann, I. J. et al. Modal aerosol dynamics model for Europe: Development and first applications. *Atmos. Environ.* **32**, 2981–2999 (1998).

54. Schell, B., Ackermann, I. J., Hass, H., Binkowski, F. S. & Ebel, A. Modeling the formation of secondary organic aerosol within a comprehensive air quality model system. *J. Geophys. Res.* **106**, 28275–28293 (2001).

55. Im, U. et al. Evaluation of operational online-coupled regional air quality models over Europe and North America in the context of AQMEII phase2. Part I: ozone. *Atmos. Environ.* **115**, 404–420 (2015).

56. Tuccella, P. et al. Modeling of gas and aerosol with WRF/Chem over Europe: Evaluation and sensitivity study. *J. Geophys. Res.* **117**, D03303 (2012).

57. National Centers for Environmental Prediction/National Weather Service/NOAA/U.S. Department of Commerce. *NCEP FNL Operational Model Global Surface Analyses*. Research Data Archive at the National Center for Atmospheric Research, Computational and Information Systems Laboratory. <https://rda.ucar.edu/datasets/ds083.2/> (1997).

58. Emmons, L. K. et al. Description and evaluation of the Model for Ozone and Related chemical Tracers, version 4 (MOZART-4), *Geosci. Model Dev.* **3**, 43–67 (2010).

59. Salamanca, F. & Martilli, A. A new Building Energy Model coupled with an Urban Canopy Parameterization for urban climate simulations-part II. Validation with one dimension off-line simulations. *Theor. Appl. Climatol.* **99**, 345–356 (2010).

60. Ribeiro, I., Martilli, A., Falls, M., Zonato, A. & Villalba, G. Highly resolved WRF-BEP/BEM simulations over Barcelona urban area with LCZ. *Atmos. Res.* **248**, 105220 (2021).

61. Guevara, M., Tena, C., Porquet, M., Jorba, O. & Pérez García-Pando, C. HERMESv3, a stand-alone multi-scale atmospheric emission modelling framework – Part 1: global and regional module. *Geosci. Model Dev.* **12**, 1885–1907 (2019).

62. Stewart, I. D. & Oke, T. R. Local Climate Zones for Urban Temperature Studies. *Bull. Amer. Meteor. Soc.* **B93**, 1879–1900 (2012).

63. Granier, C. et al. The Copernicus Atmosphere Monitoring Service global and regional emissions. *Copernicus Atmosphere Monitoring Service (CAMS) report*. <https://doi.org/10.24380/d0bn-kx16> (2019).

64. Guenther, A. B. et al. The Model of Emissions of Gases and Aerosols from Nature version 2.1 (MEGAN2.1): an extended and updated framework for modeling biogenic emissions. *Geosci. Model Dev.* **5**, 1471–1492 (2012).

65. Servei Meteorològic de Catalunya (SMC). Butlletí climàtic mensual Abril 2016. *Departament de Territori i Sostenibilitat*. <https://static-m.meteo.cat/wordpressweb/wp-content/uploads/2015/06/26072356/Butllet%C3%AD-abril2016.pdf> (2016).

66. Servei Meteorològic de Catalunya (SMC). Butlletí climàtic mensual Abril 2020. *Departament de Territori i Sostenibilitat*. https://static-m.meteo.cat/wordpressweb/wp-content/uploads/2021/03/01155111/Butllet%C3%AD-Abril2020_v3.pdf (2020).

67. Badia, A. et al. Metadata record for the article: A take-home message from COVID-19 on urban air pollution reduction through mobility limitations and teleworking. *Figshare* <https://doi.org/10.6084/m9.figshare.14743797> (2021).

68. National Centers for Environmental Prediction/National Weather Service/NOAA/U.S. Department of Commerce. 1997. *NCEP FNL Operational Model Global Surface Analyses*. Research Data Archive at the National Center for Atmospheric Research, Computational and Information Systems Laboratory. <https://doi.org/10.5065/978H-D239> (last access: 5 March 2020).

69. Granier, C. et al. The Copernicus Atmosphere Monitoring Service global and regional emissions. *ECCAD* <https://doi.org/10.24380/m89g-j508> (2019).

70. Badia, A. WRF-Chem output- NO₂ and O₃ concentrations for the base case and each emission scenario. *Zenodo* <https://doi.org/10.5281/zenodo.4767308> (2021).

71. Wild, O., Zhu, X. & Prather, M. J. Fast-J: Accurate Simulation of In- and Below-Cloud Photolysis in Tropospheric Chemical Models. *J. Atmos. Chem.* **37**, 245–282 (2000).

ACKNOWLEDGEMENTS

This work has been made possible thanks to the financial support of the ERC Consolidator Integrated System Analysis of Urban Vegetation and Agriculture (818002-URBAG) and the Spanish Ministry of Science, Innovation and Universities, through the “Maria de Maeztu” programme for Units of Excellence (CEX2019-000940-M).

This research has been supported by MINECO-Spain (TIN2017-84553-C2-1-R), and by the Spanish government grant PRE2018-085425. The authors thankfully acknowledge the computer resources at PICASSO and the technical support provided by the Universidad de Málaga (RES-AECT-2020-2-0004). The authors further wish to thank XVPCA for the provision of measurement stations. Also, thanks to the free use of HERMESv3_GR and the developing team for their support. We also thank the Copernicus Global and Regional emissions service for the emission inventory.

AUTHOR CONTRIBUTIONS

J.L. and G.V. devised the research. A.B., J.L. and G.V. initiated the study; A.B. developed and performed the WRF-Chem simulations and analyzed the model output. V.V. analyzed the observational datasets. A.B., J.L. and G.V. wrote the manuscript with contributions from all authors.

COMPETING INTERESTS

The authors declare no competing interests.

ADDITIONAL INFORMATION

Supplementary information The online version contains supplementary material available at <https://doi.org/10.1038/s42949-021-00037-7>.

Correspondence and requests for materials should be addressed to G.V.

Reprints and permission information is available at <http://www.nature.com/reprints>

Publisher's note Springer Nature remains neutral with regard to jurisdictional claims in published maps and institutional affiliations.



Open Access This article is licensed under a Creative Commons Attribution 4.0 International License, which permits use, sharing, adaptation, distribution and reproduction in any medium or format, as long as you give appropriate credit to the original author(s) and the source, provide a link to the Creative Commons license, and indicate if changes were made. The images or other third party material in this article are included in the article's Creative Commons license, unless indicated otherwise in a credit line to the material. If material is not included in the article's Creative Commons license and your intended use is not permitted by statutory regulation or exceeds the permitted use, you will need to obtain permission directly from the copyright holder. To view a copy of this license, visit <http://creativecommons.org/licenses/by/4.0/>.

© The Author(s) 2021